Radiotherapy and Oncology 131 (2019) 160–165

Contents lists available at ScienceDirect

Radiotherapy and Oncology

journal homepage: www.thegreenjournal.com

Original Article

Prospect of robotic assistance for fully automated brachytherapy seed placement into skull base: Experimental validation in phantom and cadaver

Jian-Hua Zhu [a], Jing Wang [a], Yong-Gui Wang [b], Meng Li [b], Xiao-Jing Liu [a,1,*], Chuan-Bin Guo [a,1,*]

[a] Department of Oral and Maxillofacial Surgery, Peking University School and Hospital of Stomatology, Beijing, PR China; and [b] Intelligent Robotics Institute, Beijing Institute of Technology

ARTICLE INFO

Article history:
Received 10 July 2017
Received in revised form 24 November 2017
Accepted 27 November 2017

Keywords:
Robot
Brachytherapy
Skull base
Navigation
Seed localization accuracy

ABSTRACT

Background and purpose: To investigate the feasibility and accuracy of robot-assisted brachytherapy for skull base tumours.

Material and methods: A custom robot system was tested on both phantom and cadaveric specimen. Cone beam CT (CBCT) images were transferred to the graphical user interface (GUI) for planning trajectories and the data were sent to the robot control unit. Following registration, the puncture needle was inserted into the target by the robot under navigation guidance, and seeds were implanted. Placement error was instantly displayed on the GUI; the result was verified after postoperative image scanning.

Results: A total of 150 seeds (100 for phantom experiments, 50 for cadaveric studies) were deposited by the robot system. In phantom experiments the mean placement error was 0.57 ± 0.21 mm (measured by the navigation system) vs. 1.41 ± 0.38 mm (measured by image fusion) ($p < 0.001$); in cadaveric studies the corresponding figures were 0.60 ± 0.30 mm vs. 2.48 ± 0.32 mm ($p < 0.001$). There was no significant difference for comparison of accuracy test in phantom experiments ($p = 0.173$) as well as in cadaveric studies ($p = 0.354$). Accuracy was better in the phantom experiment than in cadaveric studies ($p < 0.001$).

Conclusions: The performance of robot-assisted skull base brachytherapy is feasible and accurate. Dosimetric coverage will need to be demonstrated in further studies.

Brachytherapy is being increasingly accepted as an alternative treatment for cancer patients who are not suitable candidates for surgery or as a supplementary therapy after surgical resection; it benefits patients with the advantages of functional saving, symptomatic palliation and local disease control [1–3]. External radiotherapy is also an option for malignancies, but the high risk of severe side effects is a significant disadvantage [4]. In head and neck lesions – especially recurrent head and neck cancer – brachytherapy can provide high local control rate, relatively good quality of life and better protection of adjacent healthy tissues [1]. Brachytherapy is well suited for skull base tumors because, unlike traditional radiotherapy, it allows the delivery of a high radiation dose to the tumors with being less likely to harm critical organs [5]. However, it poses special problems in the head and neck region because of the structural complexity of this area; this is particularly true for the skull base and infratemporal region. Manually locating the skin entry site before needle insertion and adjusting the angulation of the needle, as well as negotiating the obstruction posed by the mandibular bone, can all be technically challenging for the surgeon. Theoretically, the curative effect highly depends on the accuracy of the seeds' implantation. Poor accuracy may seriously affect therapeutic efficacy and increase the occurrence and also result in the damage of surrounding normal tissue [6]. To date, the accuracy of seeds' implantation for the treatment of the head and neck malignancies has not been specifically explored [6]. Although existing techniques such as conventional CT guide [7], individual template assistance [2] and image navigation [8] provide considerable assistance, accurate needle placement still depends to a great extent on the surgeon's experience and hand–eye–mind coordination; besides, these techniques are all associated with staff exposure. Although there is no definite evidence that radioactive seeds' implantation can adversely affect the operator's health, the potential ill effects of radiation cannot be ignored. However, the integration of imaging

* Corresponding authors at: Department of Oral and Maxillofacial Surgery, Peking University School and Hospital of Stomatology, No. 22 Zhongguancun South Avenue, Haidian District, Beijing 100081, PR China.

E-mail addresses: zjhsd8811@163.com (J.-H. Zhu), wjing0122@163.com (J. Wang), wangyg1025@163.com (Y.-G. Wang), bitbatu@163.com (M. Li), user_ nancy@163.com (X.-J. Liu), guodazuo@vip.sina.com (C.-B. Guo).

[1] Prof. Chuan-Bin Guo and Dr. Xiao-Jing Liu have made equal intellectual contributions to the manuscript.

https://doi.org/10.1016/j.radonc.2017.11.031
0167-8140/

and robotic technology functions as "the third hand and eye" of the surgeon, enabling automatic needle insertion and seeds' delivery while keeping the surgeon at a safe distance from the radioactive seeds; it does away with the need for the surgeon to repeatedly switch vision between the patient and the monitor [9].

Several robot systems for brachytherapy have been reported, but most have been for the treatment of prostate and lung cancers [3]. Although robot-assisted surgery has been applied in oral and maxillofacial surgery (OMFS) for procedures such as transoral robotic surgery [10] and assistant orientation for reconstructive surgery [11], its use for brachytherapy in the field of OMFS is hardly reported. We have developed a custom robot system for skull base and infratemporal region tumors' biopsy [12], which was transformed to perform automatic seeds' implantation in this study. We evaluated the feasibility and reliability of this robot system in phantom experiments and cadaveric studies, which is the necessary component for introducing a novel equipment into clinical practice.

Materials and methods

Experimental setup

The robot device comprises an arch-like structure, with a positioning mechanism for needle orientation and an end effector for seeds' delivery (Fig. 1). It is remote controlled and portable, weighing only 15 kg, and can be easily fixed to the operating table. In brief, the technical specifications of the robot system include the following: (1) 6-degrees of freedom (DOF), i.e., 3 DOF for rotational motions, 1 DOF for horizontal motion, 1 DOF for radial motion and seeds' implantation; (2) 55 cm × 20 cm (width × height), which was chosen after taking into consideration the configuration of the operation table and the need for easy cleaning of the parts; (3) an end effector containing a cartridge with seeds was connected to the fifth joint by a clamping slot connection, which facilitated easy removal and sterilization; (4) a 300 × 400 × 400 mm (x, y, z) three-dimensional workspace; (5) an optical tracking system (Polaris; Northern Digital Inc., Waterloo, Canada) with 0.35-mm positioning accuracy and 20-Hz update rate; (6) a custom user-friendly graphical user interface (GUI) for robot control, workflow tracking and safety guarantee; (7) a custom software for preoperative surgical planning and registration, intraoperative real-time navigation and postoperative validation; and (8) a 6-dimension force sensor (3813A SRI; Sunrise Instruments, Nanning, China) placed between the fifth joint and the end effector.

In the phantom experiment, 3 synthetic human skulls (A150; Kexin Scientific Equipment, Zhangjiagang, China) were used. Plasticine® was placed around the skull base to imitate soft tissue. Oval masses (made by beef) of 3 cm diameter were placed beneath the skull base to act as the target "tumours". In the cadaveric study, 2 formalin-preserved human heads (1 male, 1 female) were obtained from the Anatomy Department of our institute. Iopamidol (370 mg/mL; Bracco Sine Limited, Shanghai, China) was injected into different areas in the skull base and infratemporal region, and the tissues containing the injected dye acted as the "tumours" in the cadaveric study. Stainless steel wires of 1 mm diameter and 5 mm length were used instead of radioactive seeds in all experiments to avoid radiation exposure to the investigators. We planned to implant 30 seeds, 30 seeds and 40 seeds for 3 skull phantoms respectively and 25 seeds for each cadaver. The study was approved by the local ethics committee.

Workflow

Image scanning

Preoperative cone beam CT (CBCT) scanning was performed using a NewTom VG scanner (Quantitative Radiology, Verona, Italy). The CBCT data (110 kV, 13.88 mA, field-of-view 15 cm × 15 cm, matrix 512 × 512, slice thickness 0.3 mm) was transferred to the computer console in DICOM (Digital Imaging and Communications in Medicine) format and displayed on a custom GUI for the surgical planning and registration.

Surgical planning

After segmentation of the "tumour" image data, the seeds' distribution including the seed positions and orientations was calculated. Once the location of the seeds was specified on the GUI, the trajectory of the needle was automatically selected by the software. The relevant data were calculated and sent to the robot controller by socket communication through the local area network.

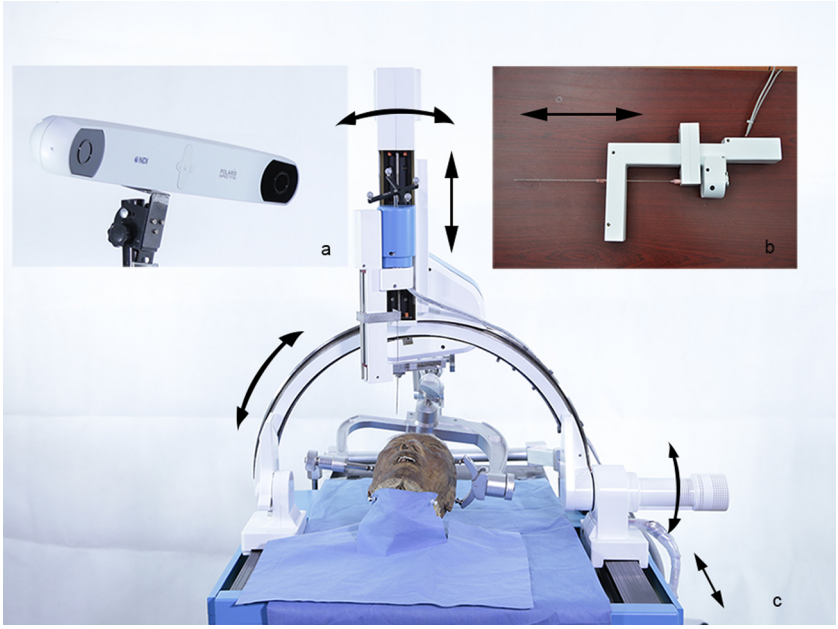

Fig. 1. Overview of the robot system with 6 DOF (black arrows): the optical tracking system (a), the end effector (b), and the robot device (c).

Navigation registration

The navigation system and the robot were first initialized. Before imaging was performed, nine titanium screws of 2-mm diameter (Synthes, Solothurn, Switzerland) were inserted around the craniomaxillofacial region to act as fiducial markers; this collection of paired points has been recommended by Caversaccio [13]. The fiducial markers showed on the image data were manually selected on the GUI by a mouse and the corresponding coordinates of the fiducial markers on the skull could be located by the probe of the navigation system. The intraoperative registration of the phantom or cadaver skull to the images was performed by means of the paired point method through the corresponding fiducial markers, using an improved iterative closest point (ICP) algorithm [14]. The registration of the robot to the tracking system was also performed by the point-based method with the inherent points in the robot arm. The images, patient, and robot were then aligned by matrix transformation. The optical tracking system, as an intermediate coordinate, was used to correlate the different coordinate systems. After the registration of robot to the tracking system, all movements of the robot system were guided by the optical navigation system through the closed-loop control strategy, with a permissible location error of only 0.01 mm (Fig. 2); the registration error was verified visually by comparison with a calibrated standard model.

Needle positioning and seed delivery

Once the preoperative planning was confirmed, the relevant intraoperative needle orientation data and the coordinates of planning seeds ($X1$, $Y1$, $Z1$) were calculated and sent to the robot controller. The robot, with an 18-gauge needle (150 mm; MTP-1820-C; Hakko Co., Ltd., Japan) clamped in the end effector, was driven to the target position automatically along the planned straight trajectory. The imaging feedback was displayed in real time on the navigation interface through continuous updating of the needle orientation data acquired by the optical tracking system. The interactive control system unit was designed as a "man-in-closed-loop" mode – with inclusion of the imaging data, tracking system, robot, and surgeon – to provide double feedback for calibrating and monitoring the process. Thus, when the needle was at the entry point, the robot would remain motionless, and would advance the needle further only after receiving confirmation from the surgeon. During intervention process, any axial force transferred to the force sensor was displayed on the GUI after signal translation; this served to alert accidental collision of the needle with bone for safety consideration. When the needle tip was in position, the seed pressed in the cartridge of the end effector was rebounded into the cannula, and then the stylet was automatically driven by the sixth DOF to push the seed to the target point.

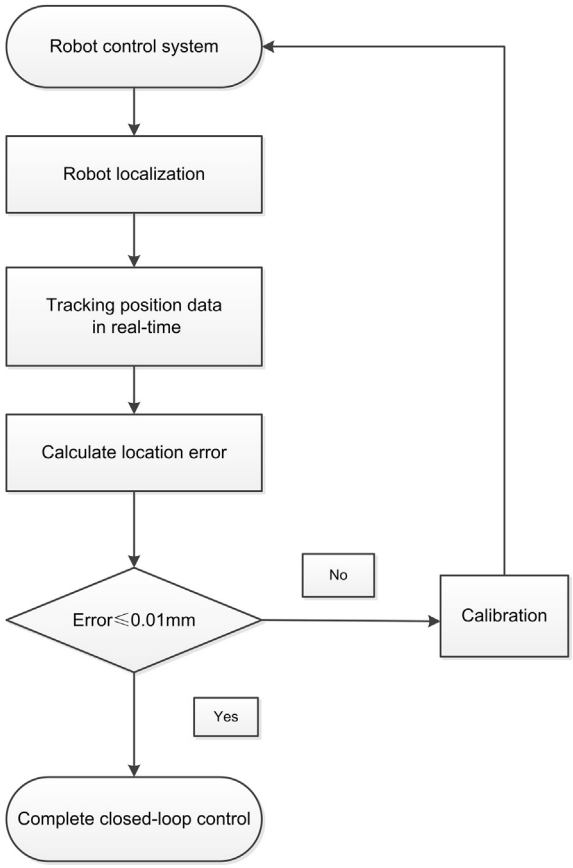

Fig. 2. Closed-loop control (the position data of the needle tip was acquired by the navigation system in real-time and the corresponding localization error was calculated by robot control unit. The targeting result was supposed to be achieved until the error value less than 0.01 mm).

Postoperative imaging

On completion of the intervention procedure, the instantaneous data of needle orientation acquired by the navigation system was sent back to the GUI for postoperative accuracy verification. After the seeds had been delivered, imaging (Fig. 3) was also performed to verify the position of the seeds with the same CBCT setup. The preoperative planning coordinates ($X1$, $Y1$, $Z1$) and the postoperative ($X2$, $Y2$, $Z2$) seeds' position were aligned by matrix transformation after image fusion, whose systematic error was 0.01 mm using modified ICP algorithm [15]. The total error was defined as the Euclidean distance ($\sqrt{\Delta X^2 + \Delta Y^2 + \Delta Z^2}$) calculated by the offsets of the coordinates, which was taken as the gold standard.

Statistical analysis

Statistical analysis was performed using IBM SPSS for Windows, Version 20 (IBM Corp., Armonk, NY, USA). The paired t test was used to compare the accuracy of seed implantation measured by the navigation system and by postoperative verification. Statistical significance was set at $p \leq 0.05$. The One-Way ANOVA was used to compare the accuracy of seed implantation among 3 skulls in phantom experiments (30 seeds, 30 seeds and 40 seeds for 3 skull phantoms respectively). Statistical significance was set at $p \leq 0.05$. The Independent Samples Test was used to compare the accuracy of seed implantation between 1 male and 1 female in cadaveric studies (25 seeds for each cadaver). Statistical significance was set at $p \leq 0.05$. The Mann–Whitney U test was used to compare the accuracy of seed implantation and insertion depth between phantom experiments and cadaveric studies. Statistical significance was set at $p \leq 0.05$. The Pearson Correlation Coefficients (r) was used to analyse correlation between the accuracy of seed implantation and insertion depth in phantom experiments and cadaveric studies.

Results

All planned seeds could be inserted. A total of 150 seeds (100 for phantom experiments and 50 for cadaveric studies) were deposited by the robot system (Table 1 and Fig. 4). The placement errors measured by the navigation system were statistically significantly different from the error values calculated by image fusion in phantom experiments ($p < 0.001$) as well as in cadaveric studies ($p < 0.001$). The comparison of accuracy test showed no significant difference in both phantom experiments ($p = 0.173$) and cadaveric studies ($p = 0.354$), but there was a significant difference between

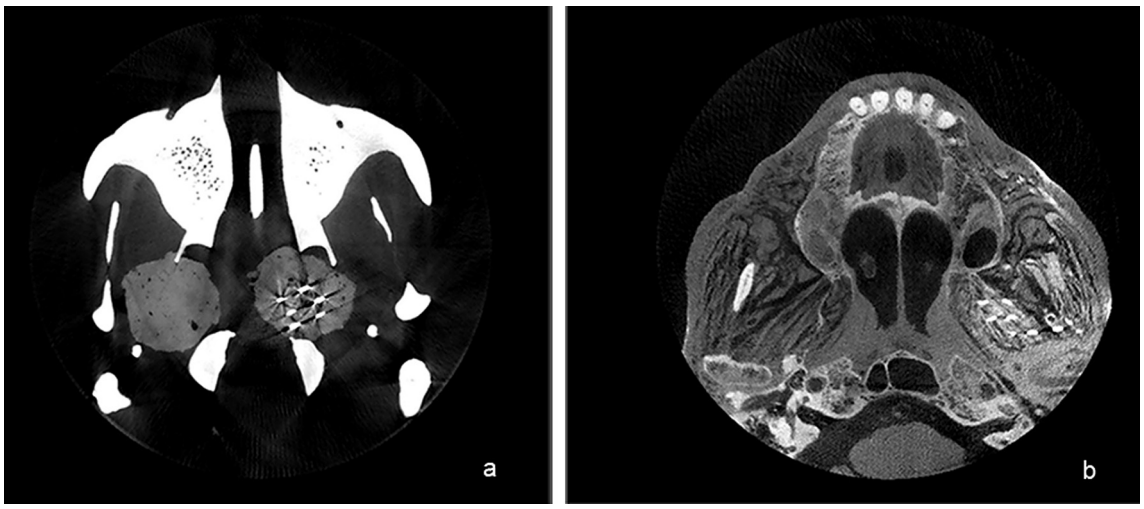

Fig. 3. Postoperative images of the phantom experiment (a. seeds implanted into the neoplasm beneath the left skull base) and the cadaveric study in different level (b. seeds located in target area with injected dye beneath the left skull base).

Table 1
Accuracy measured by navigation system and image fusion (determined by 0.35 mm voxel CBCT system and 0.01 mm systematic error) and insertion depth of robot-assisted seeds' implantation guided by optical navigation.

Method	Number of seeds' implanted	Accuracy (mm)		Depth (mm)
		Measured by navigation system Mean ± Standard deviation (Minimum, Maximum)	Measured by image fusion Mean ± Standard deviation (Minimum, Maximum)	Mean ± Standard deviation (Minimum, Maximum)
Phantom	100	0.57 ± 0.21 (range: 0.3–0.93)	1.41 ± 0.38 (range: 0.46–1.92)	43.64 ± 6.55 (range: 30.11–55.57)
Cadaver	50	0.60 ± 0.30 (range: 0.1–1.37)	2.48 ± 0.32 (range: 1.79–2.96)	44.52 ± 6.74 (range: 30.46–56.42)

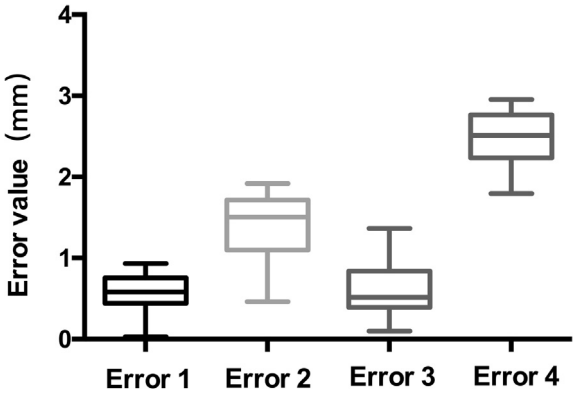

Fig. 4. The mean errors, minimum errors and maximum errors measured by the navigation system (error 1) and by image fusion (error 2) in phantom experiment and the cadaveric study (errors 3 and 4).

phantom experiments and cadaveric studies ($p < 0.001$). The seeds' implantation in the phantom experiments was significantly more accurate than in the cadaveric studies at a comparable insertion depth ($p = 0.550$). The r was 0.306 and 0.676 in phantom experiments and cadaveric studies respectively. It needed 40 min to implant 30 seeds.

Discussion

Optical navigation has been routinely used in clinical interventions as it provides real-time vision feedback by continuous updating of the instrument position. In view of the risk of radiation exposure associated with intraoperative CT guidance and the disadvantage of the image artifacts arising from the robot metallic components, optical navigation could be considered the optimal alternative for guided interventions, with benefits to both patients and surgeons during local therapy of skull base lesions. In this preliminary study, location accuracy and real-time image feedback for safety depend on uninterrupted updating of position data acquired by optical tracking, and therefore, the low data acquisition frequency of the optical localizer is the main hurdle to increasing intervention speed, which can potentially improve targeting accuracy [16]. The problem posed by the line of sight between the camera and the infrared markers is another non-negligible drawback with optical navigation [17]. Electromagnetic tracking, with the sensor attached to the needle tip, is another potential navigation system for monitoring needle interventions [18]; however, the use of electromagnetic tracking in this system was precluded by the fact that the robot parts were of ferromagnetic material; furthermore, electromagnetic tracking has been reported to have a relatively low location accuracy in the interventional realm [17].

Several researchers have reported the accuracy of needle intervention for brachytherapy. In previous studies, different materials have been used to simulate soft tissues, with most studies using gels and polyvinyl chloride, which cannot really simulate the complexity of the tissues of the head and neck region [2]. Indeed, in our research, the primary phantom study had the same limitation, as neither Plasticine® nor the meat balls used as targets exhibit significant anisotropy or simulate the complex behaviour of soft tissues. The needle tip location error measured by the navigation system was significantly different from the seeds' location error measured

by postoperative verification ($p < 0.001$); the average difference was 0.84 ± 0.39 mm (range: 0.12–1.73 mm). Some factors such as image distortion and human error [19] are uncontrollable; if these are disregarded, accuracy is affected largely by navigation errors [12] and seeds' displacement [20] in this case, where nonelastic Plasticine®, a relatively stiff needle, and close-loop control strategy with submillimeter accuracy were introduced. Actually, there are no major variations in resistance when the stylet is advanced through nonelastic material, and migration of seeds due to tissue reaction is negligible. Navigation errors consist of registration errors and optical localizer errors (0.35-mm accuracy); this may have contributed considerably to the location error identified in our phantom study. The target registration error in the lateral skull base varies from 0.1 to 1.8 mm [13]. Kettenbach et al. calculated the fiducial registration error to validate the quality of the registration before needle insertion [21]. However, given that the fiducial registration error is small, there can still be a large target registration error [17]. After registration of the robot to the navigation system, the motion accuracy of the robot was restricted to within submillimeter by the closed-loop control strategy. However, a limitation of the study is that only visual feedback was used for verification. The system accuracy of the needle tip location guided by the navigation consisted of registration errors (0.1–1.8 mm), optical localizer errors (0.35 mm) and the limitation of motion control algorithm (0.01 mm). In reality, it is hardly practical to separate the contribution of each component, and to quantify them for every time. The total error is not just a sum of the errors of each components, it even may be below the summation [22]. The difference of the accuracy measured by the two methods was also statistically significant ($p < 0.001$) in the cadaveric study; the average difference was 1.88 ± 0.44 mm (range: 1.08–2.67 mm). Additionally, it should be noted that seeds' implantation in the phantom experiment was more accurate than in the cadaveric study ($p < 0.001$) at comparable insertion depth ($p = 0.55$). But the accuracy of seed implantation among 3 skulls in phantom experiments ($p = 0.173$) was not significantly different and there was also no significant difference between the 2 human heads in cadaveric studies ($p = 0.354$). The Pearson Correlation Coefficients (r) showed the close correlation between the accuracy of seed implantation and insertion depth in cadaveric studies (0.676) while it is weaker (0.306) in phantom experiments. A reasonable explanation is that needle deflection was primarily responsible for needle displacement within real tissues, as has been reported in previous studies [5,23,24]. Although the closed-loop control guarantees robot motion accuracy to within 1 mm, the performance of needles, which are vulnerable to be bendable, can introduce external errors for an optical tracking system; it is the hurdle for the fine calibration of the location offsets. Theoretically, the answer to needle deflection is to make compensation for this in advance – i.e., during the planning stage – by creating a theoretical model for estimating needle–tissue interaction [25]. Unfortunately, although many efforts have been made to model needle insertion forces [26–28], it has so far not been possible to correctly predict needle–tissue interactions because of the variability of soft tissues properties [16]. Technically, it is the imbalance of the forces applied to the surface of the asymmetric needle tip that causes needle deflection [29]. Interventions with rotating needles can produce lateral friction forces that can overcome needle deflection, but this would be at the cost of increased trauma [5,30,31]. As a compromise, rotating after needle insertion is a considerable alternative to provide highly beneficial accuracy at relatively low cost [16], and we will take this into consideration when designing the next generation of the robot system. In the cadaveric study, we observed slight slippage of the needle tip (nearly 1 mm needle tip deviation) at the moment when the needle tip pierced the skin, especially in cases where an oblique trajectory was planned; it was also a possible explanation for the close correlation between the seed accuracy and insertion depth in cadaveric studies. Actually the intrabody deflection was more influential than entering slippage for the final seed accuracy because when the position of the entry point changed (caused by the slippage effect), the correction was instantly performed by the closed loop control unit guided by the navigation until the location error below the defined threshold. After that, the needle was advanced further. In fact, the correction effect was based on the assumption that the needle was nonflexible and rigidly connected with the robot end effector, while the needle deflection was the limitation for the navigation to improve position accuracy. Planning a trajectory perpendicular to the skin should help reduce needle displacement during skin penetration. To reduce needle deflection further, a relatively stiff needle with a diamond needle tip can be used. Small incisions at the selected puncture site will also facilitate needle advancement without deflection [32,33]. In addition, the released seeds can drift when there is relaxation of stressed tissues as the needle is withdrawn; therefore, relatively slow retraction of the needle and efforts to keep the trocar stable can also reduce seeds' displacement [20]. In this study, the speed of needle insertion and retraction is 3 mm/s and it is adjustable according to clinic application.

Robotic assistance for brachytherapy has been a field of active research [3,20,23,30,34,35]. However, it is arguably difficult to compare the performance of our robot system with those existing robot systems as the latter have mostly been applied for prostate and lung brachytherapy; the other systems are developed for different purposes with distinctive technologies. For example, Song et al. performed the first *in vivo* trial for robotic prostate brachytherapy where they demonstrated the submillimeter errors of the robot detected by the same POLARIS™ system as we used, and the advantage of US guidance in making fine adjustments to correct needle deflection [35]. Unfortunately, US guidance is not feasible in the skull base and infratemporal regions because of the surrounding bony structures, with the mandibular bone making access particularly difficult. Besides, manual needle insertion would defeat the purpose of having a "fully automated" robotic system for brachytherapy. Ma et al. compared robot-assisted thoracoscopic brachytherapy with manual seed implantation for lung cancer and surprisingly found worse accuracy with the robot system [36]. In their opinion, the long learning curve and the absence of image guidance and navigation techniques may have contributed to the disappointing performance. Additionally, no standard for seeds' implantation accuracy has been defined for routine clinical practice. The accuracy of 3–6 mm *in vivo* is estimated with manual seed placement [9], than which we want to achieve a better accuracy using robotic technique to protect staff from radiation exposure. The accuracy of 2 mm is clinically acceptable compared with manual procedure in expert clinical opinion for robot-assisted lung brachytherapy [18]. Unfortunately, as far as we know, there is no specific accuracy value for skull base brachytherapy. In this study, we wanted to achieve more accurate seed placement than 3 mm performed by manual technique. Pappas et al. developed a navigation system with a mechanical positioning device for brachytherapy of frontal skull base tumors, and achieved 1.4-mm positioning accuracy in a phantom experiment, which is similar to our results [5]. Different from other interventions such as biopsy and ablation, the seeds' implantation deviation tolerances depend on the dosimetric coverage. Nath et al. investigated the dosimetric effects of needle divergence in prostate seed implant, suggesting that the deviation should be kept within 5 mm to ensure that reduction in dose to the target area would be <5% [37]. In our future research, we intend to study how seeds' displacement affects dose distribution in the head and neck region and to quantify the dosimetric loss, even compare the dose distribution and time with manual technique; this is an

important factor in deciding treatment outcome and quality of life of patients [34]. The use of 1D or 2D TG-43 formalism, as well as specification of source strength with a traceable quantity such as reference air kerma rate (RAKR) should also be concerned. Besides, compared with the conventional process (10 min for 30 seeds), the robot-assisted brachytherapy (40 min for 30 seeds) needed extra half-hour to make accurate registration of the patient, imaging, navigation and robot at the beginning, but the duration of the procedure would be shortened with increasing experience.

Conclusions

In this preclinical evaluation, the robot system for automatical seeds' implantation under optical tracking guidance demonstrated encouraging results. Accuracy of seed placement was better in the phantom experiments (1.41 ± 0.38 mm) than in cadaveric studies (2.48 ± 0.32 mm). Navigation accuracy and needle deflection are significant factors in robotic interventions. The intraoperative location error measured by optical tracking is not reliable, and postoperative image verification is necessary. Further research on post-implantation dosimetry is also necessary before this method can be introduced into clinical practice.

Conflicts of interest statement

All authors declare no financial and personal relationships with other people or organisations.

Acknowledgments

This work was funded by the National High-Tech R&D Program (863 Program) of China [grant number 2012AA041606] and the Beijing Science and Technology Project, China [grant number Z141100002014003].

References

[1] Wierzbicka M, Bartochowska A, Strnad V, et al. The role of brachytherapy in the treatment of squamous cell carcinoma of the head and neck. Eur Arch Otorhinolaryngol 2016;273:269–76.
[2] Huang MW, Zhang JG, Zheng L, Liu SM, Yu GY. Accuracy evaluation of a 3D-printed individual template for needle guidance in head and neck brachytherapy. J Radiat Res 2016;57:662–7.
[3] Popescu T, Kacso AC, Pisla D, Kacso G. Brachytherapy next generation: robotic systems. J Contemp Brachytherapy 2015;7:510–4.
[4] Tselis N, Karagiannis E, Kolotas C, Baghi M, Milickovic N, Zamboglou N. Image-guided interstitial high-dose-rate brachytherapy in the treatment of inoperable recurrent head and neck malignancies: an effective option of reirradiation. Head Neck 2017;39:E61.
[5] Pappas IP, Ryan P, Cossmann P, Kowal J, Borgeson B, Caversaccio M. Improved targeting device and computer navigation for accurate placement of brachytherapy needles. Med Phys 2005;32:1796–801.
[6] Huang MW, Liu SM, Zheng L, et al. A digital model individual template and CT-guided 125I seed implants for malignant tumors of the head and neck. J Radiat Res 2012;53:973–7.
[7] Jiang YL, Meng N, Wang JJ, et al. CT-guided iodine-125 seed permanent implantation for recurrent head and neck cancers. Radiat Oncol 2010;5:68.
[8] Krempien R, Hassfeld S, Kozak J, et al. Frameless image guidance improves accuracy in three-dimensional interstitial brachytherapy needle placement. Int J Radiat Oncol Biol Phys 2004;60:1645–51.
[9] Podder TK, Beaulieu L, Caldwell B, et al. AAPM and GEC-ESTRO guidelines for image-guided robotic brachytherapy: report of Task Group 192. Med Phys 2014;41:101501.
[10] De Ceulaer J, De Clercq C, Swennen GR. Robotic surgery in oral and maxillofacial, craniofacial and head and neck surgery: a systematic review of the literature. Int J Oral Maxillofac Surg 2012;41:1311–24.
[11] Zhu JH, Deng J, Liu XJ, Wang J, Guo YX, Guo CB. Prospects of robot-assisted mandibular reconstruction with fibula flap: comparison with a computer-assisted navigation system and freehand technique. J Reconstr Microsurg 2016;32:661–9.
[12] Zhu JH, Wang J, Wang YG, et al. Performance of robotic assistance for skull base biopsy: a phantom study. J Neurolog Surg B Skull Base 2017;78:385.
[13] Caversaccio M, Zulliger D, Bachler R, Nolte LP, Hausler R. Practical aspects for optimal registration (matching) on the lateral skull base with an optical frameless computer-aided pointer system. Am J Otol 2000;21:863–70.
[14] Bae KH, Lichti DD. A method for automated registration of unorganised point clouds. ISPRS J Photogramm 2008;63:36–54.
[15] Xie Z, Xu S, Li X. A high-accuracy method for fine registration of overlapping point clouds. Image Vis Comput 2010;28:563–70.
[16] Badaan S, Petrisor D, Kim C, et al. Does needle rotation improve lesion targeting? Int J Med Robot 2011;7:138–47.
[17] Masamune K, Hong J. Advanced imaging and robotics technologies for medical applications. Int J Optomechatron 2011;5:299–321.
[18] Lin AW, Trejos AL, Mohan S, et al. Electromagnetic navigation improves minimally invasive robot-assisted lung brachytherapy. Comput Aided Surg 2008;13:114–23.
[19] Kettenbach J, Kronreif G. Robotic systems for percutaneous needle-guided interventions. Minim Invasive Ther Allied Technol 2015;24:45.
[20] Fichtinger G, Burdette EC, Tanacs A, et al. Robotically assisted prostate brachytherapy with transrectal ultrasound guidance – phantom experiments. Brachytherapy 2006;5:14–26.
[21] Kettenbach J, Kara L, Toporek G, Fuerst M, Kronreif G. A robotic needle-positioning and guidance system for CT-guided puncture: ex vivo results. Minim Invasive Ther Allied Technol 2014;23:271–8.
[22] Seifabadi R, Cho NB, Song SE, et al. Accuracy study of a robotic system for MRI-guided prostate needle placement. Int J Med Robot 2013;9:305–16.
[23] Li G, Su H, Shang W, et al. A fully actuated robotic assistant for MRI-guided prostate biopsy and brachytherapy. Proc SPIE Int Soc Opt Eng 2013;8671:867117.
[24] Wan G, Wei Z, Gardi L, Downey DB, Fenster A. Brachytherapy needle deflection evaluation and correction. Med Phys 2005;32:902–9.
[25] Dogangil G, Davies BL, Rodriguez y Baena F. A review of medical robotics for minimally invasive soft tissue surgery. Proc Inst Mech Eng H 2010;224:653–79.
[26] Kataoka H, Washio T, Audette M, Mizuhara K. A model for relations between needle deflection, force, and thickness on needle penetration. In: Paper presented at: Medical image computing and computer-assisted intervention – Miccai 2001, International conference, Proceedings 2001, October 14–17, Utrecht, The Netherlands; 2001.
[27] Okamura AM, Simone C, O'Leary MD. Force modeling for needle insertion into soft tissue. IEEE Trans Biomed Eng 2004;51:1707–16.
[28] Simone C, Okamura AM. Modeling of needle insertion forces for robot-assisted percutaneous therapy. In: Paper presented at: IEEE international conference on robotics and automation; 2000.
[29] Majewicz A, Wedlick TR, Reed KB, Okamura AM. Evaluation of robotic needle steering in ex vivo tissue. IEEE Int Conf Robot Autom 2010;2010:2068–73.
[30] Davies BL, Harris SJ, Dibble E. Brachytherapy – an example of a urological minimally invasive robotic procedure. Int J Med Robot 2004;1:88–96.
[31] Meltsner MA, Ferrier NJ, Thomadsen BR. Observations on rotating needle insertions using a brachytherapy robot. Phys Med Biol 2007;52:6027–37.
[32] Abolhassani N, Patel R, Moallem M. Needle insertion into soft tissue: a survey. Med Eng Phys 2007;29:413–31.
[33] Strassmann G, Olbert P, Hegele A, et al. Advantage of robotic needle placement on a prostate model in HDR brachytherapy. Strahlenther Onkol 2011;187:367–72.
[34] Muntener M, Patriciu A, Petrisor D, et al. Magnetic resonance imaging compatible robotic system for fully automated brachytherapy seed placement. Urology 2006;68:1313–7.
[35] Song DY, Burdette EC, Fiene J, et al. Robotic needle guide for prostate brachytherapy: clinical testing of feasibility and performance. Brachytherapy 2011;10:57–63.
[36] Ma GW, Pytel M, Trejos AL, et al. Robot-assisted thoracoscopic brachytherapy for lung cancer: comparison of the ZEUS robot, VATS, and manual seed implantation. Comput Aided Surg 2007;12:270–7.
[37] Nath S, Chen Z, Yue N, Trumpore S, Peschel R. Dosimetric effects of needle divergence in prostate seed implant using ^{125}I and ^{103}Pd radioactive seeds. Med Phys 2000;27:1058–66.